UFR SCIENCES ET TECHNIQUES BESANÇON

femto-st SCIENCES & TECHNOLOGIES

EGO EUROPEAN GRAVITATIONAL OBSERVATORY

MEMOIRE

Pour obtenir le diplôme

MASTER 2ème année

SCIENCES, TECHNOLOGIE, SANTÉ

Mention
Sciences de la Matière

SPÉCIALITÉ

Photonique, mIcro&nanoteChnologies et tempS fréquence

Developpement et caractérisation d'un analyseur de spectre optique haute résolution

par

Vincent PECHEUR

Soutenu le 08/07/2016 devant le jury :

Fabrice DEVAUX
Remo GIUST
Eric LANTZ
Mathieu CHAUVET

Résumé

Ce stage a pour but le développement et la caractérisation d'un analyseur de spectre optique haute résolution dans le cadre du contrôle de l'interféromètre VIRGO. Nous parlerons de la nécessité d'un analyseur de spectre haute résolution. Nous allons détailler la construction ainsi que la procédure d'alignement de la cavité optique. Puis nous présenterons les résultats et les travaux futures.

- Cavité optique
- Travail expérimental
- Détection ondes gravitationnelles

Abstract

The produce of the trainneship is the development and the characterization of high resolution optical spectrum analyzer in order to control the interferometer VIRGO. We will discuss about the necessity of a high resolution spectrum analyzer. We will detail how we built and aligned the optical cavity. We will show results and possible future works.

- Optical cavity
- Experimental work
- Gravitational waves detection

Acknowlgments

First I would like to thank Eric GENIN who give the opportunity to do this traineeships as all members of the optics group their help. I would like to praise everybody's patience during the administrative procedure. It wasn't easy. I also have to apologize to Gary, Annalisa, Martin, Matteo and Antonino who went under the ping pong table because of my weakness.

Grazie mille a tutti.

Glossary

- **EOM**: Electro-optic modulator
- **FINESSE**:Frequency domain INterfErometer Simulation SoftwarE (http://www.gwoptics.org/)
- **FSR**: Free Spectral range
- **FWHM**: Full Width at Half Maximum
- **SFP**: Scanning Fabry-Perot
- **SFPI**: Scanning Fabry-Perot Imager
- **RF**: Radio Frequency

Contents

1 Introduction

EGO, European Gravitational Observatory, is a consortium created by CNRS (Centre National de la Recherche Scientifique) and INFN (Istituto Nazionale di Fisica Nucleare) to ensure the commissioning of the VIRGO antenna for gravitational waves, its operation, maintenance and upgrades.

VIRGO is a gravitational waves detector. It is based on a Michelson interferometer with 3 km long arms. Mirrors are placed at the extremities of each arms in order to reach an optical equivalent length of 120 km. EGO and VIRGO are based in Cascina in Italy.

The detection is done on a dark fringe, it means all the power go back to the laser. We also use a mirror at the input of VIRGO to recycle the power reflected by the interferometer. (See fig. 1.) All these mirrors forms cavities. In order not to lose power, all the cavities need to be kept at resonance.

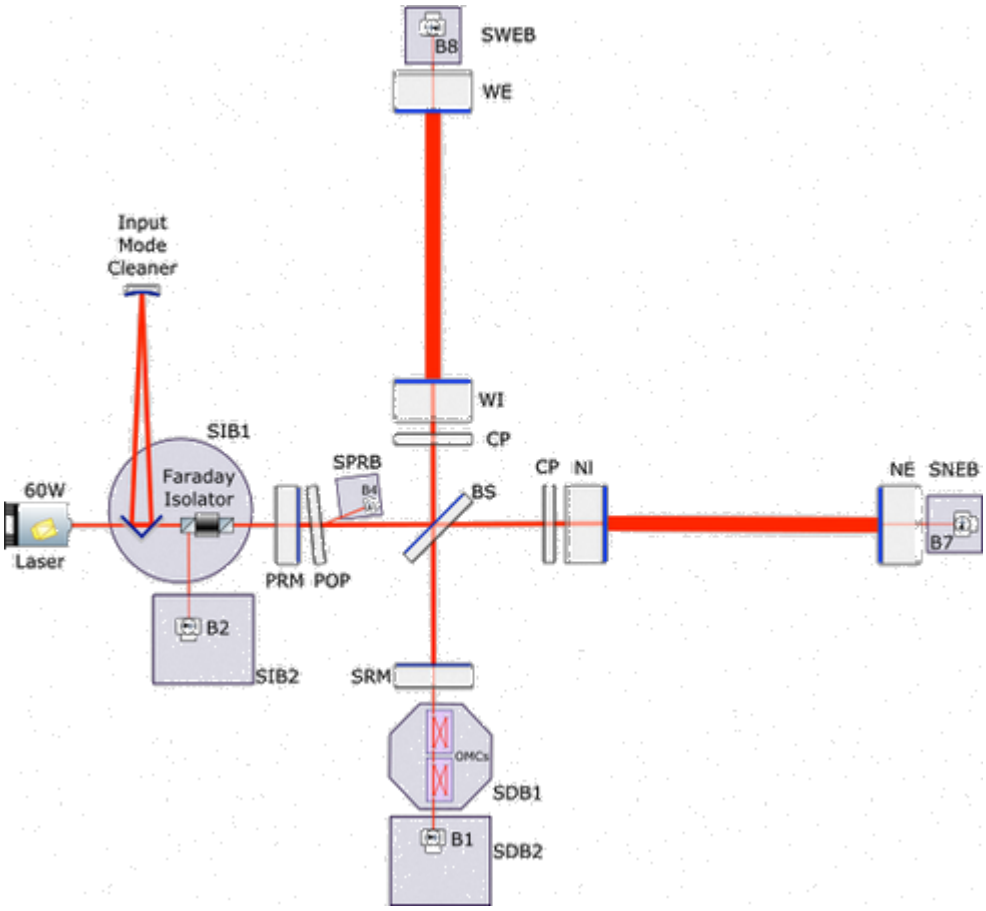

Figure 1: Layout of Advanced VIRGO

The length of each cavities has to be adjusted because of fluctuation of the laser frequency and environment perturbations. This process is called locking.

To lock cavities Pound-Drever-Hall method is used [1]. Basically the method consists in a feedback a correction on the mirrors. This correction is computed from an error signal in the reflection of the cavity to be controlled. If only use the reflected intensity, the system can't tell on which side of the resonance it is. But the derivative

of the reflected intensity is antisymmetric about the resonance and can be used as an error signal for the feedback. Fortunately, we can use a trick to get the right error signal. If we modulate the laser frequency over a small range, the reflected light will also vary. Above the resonance, the derivative is positive when the laser frequency increases, however below the resonance the derivative is negative. By comparing the variation in the reflected intensity with the frequency variation we can tell which side of resonance we are on. In practice we modulate the phase of the beam with an electro-optic modulator because it is easier to modulate the phase instead of the frequency and results are the same [2]. The reflected beam is picked off and sent to a photo-diode, whose output is compared with the oscillator we used to modulate the beam via a mixer (See fig. 2). In fig. 2, we can see a photo-diode in transmission of the cavity, it is used as a trigger. When the power reach a certain level then the locking process is turned on. We can use the error signal to drive an actuator in order to change the length of the cavity. We need more than one radio frequency (RF) if we want to lock every cavities. For example to lock arms, RF sidebands need to resonate in the cavity formed by PRM, NI and WI (See fig. 1). In practice we use four different modulation frequencies in order to lock every cavities in Advanced Virgo. [3]

This method is also used to stabilize laser frequency, the only difference being that the feedback is done on the laser instead of the cavity.

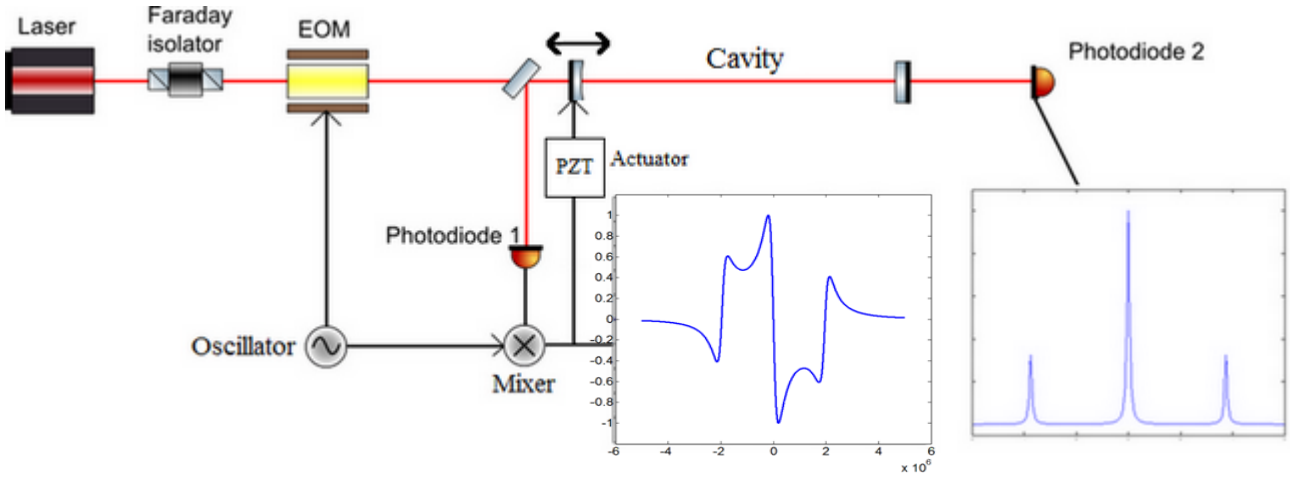

Figure 2: Basic setup for locking a cavity to a laser. Red lines are optical paths and black lines are signals.

Usually sidebands are balanced but inside a recycled interferometer like Virgo we can observe some asymmetry between sidebands. Asymmetric sidebands give us information about the asymmetry of the Michelson interferometer [4]. Due to high power laser, there are thermal effects on mirrors and the radius of curvature change. We illuminate mirrors with a CO_2 laser to compensate the distortion done by YAG laser. If the CO_2 correction is not well done on one mirror we can see that sidebands do not have the same amplitude. We can also balance sidebands by applying an offset on the error signals as done in the past for VIRGO [5](See fig. 3). It will change the working point of the feedback, it also means the cavity will not be locked perfectly on the maximum of transmission so we lose power. We need to find a compromise between sidebands balance and power losses. In general, it is preferable

to compensate the spurious effect instead of adding offsets.

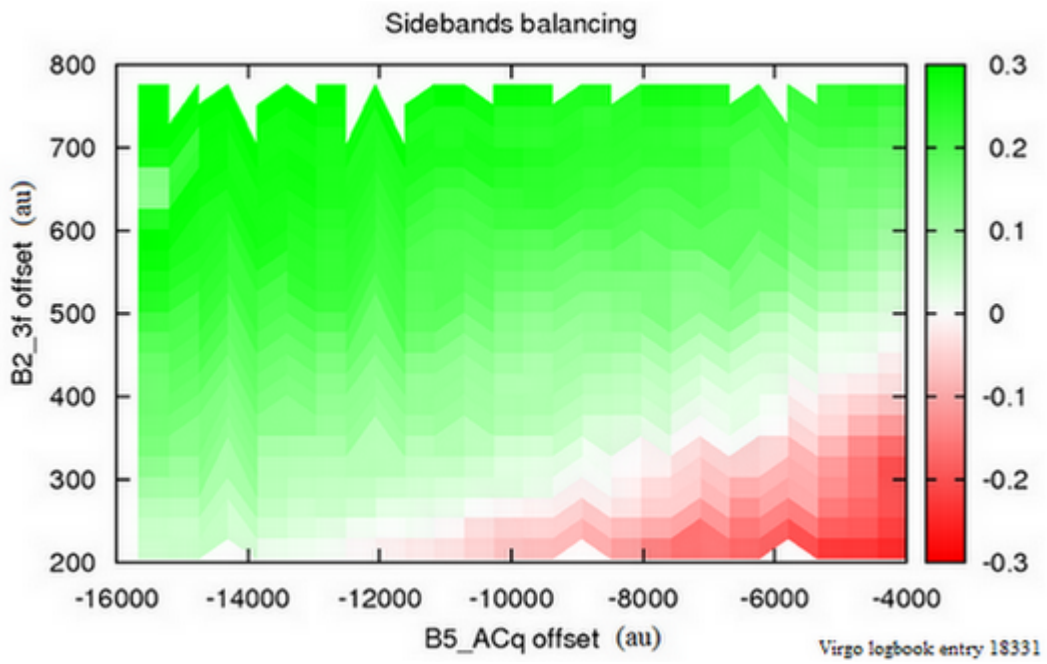

Figure 3: Balancing between sidebands in function of 2 offsets on errors signals used to keep 2 VIRGO cavities locked.

The purpose of my traineeship is to build and characterize a scanning Fabry-Perot in order to clearly resolve the four RF sidebands used to lock Virgo's cavities and check potential asymmetries of the sidebands amplitude.

2 Scanning Fabry Perot (SFP)

2.1 Theoretical part

A scanning Fabry-Perot cavity is used as a spectrometer. One mirror is mounted on a piezoelectric actuator in order to change a bit the length of the cavity, using this we can scan the free spectral range of the cavity and see every mode which can resonate. Usually 2 mirrors cavities are used to build a SFP because it is easier to align.

The main difference between all of there cavities is the degeneracy of high order gaussian modes. Generally transversal modes do not resonate at the same frequency. (See fig. 5.) The resonance frequency in a 2 mirrors cavity is given by [6] :

$$\nu_{qnm} = [q + (n + m + 1) \cdot \frac{cos^{-1}(\pm\sqrt{g_1 g_2})}{\pi}] \cdot \frac{c}{2L} \tag{1}$$

with $g_1 = 1 - \frac{L}{R_1}$, $g_2 = 1 - \frac{L}{R_2}$, L the length of the cavity, $R_{1,2}$, mirrors radius of curvature. q index is used for longitudinal modes and n,m for transversal modes. In Eq. 1 we apply the sign + when g_1 and g_2 are positive otherwise the sign - is used.

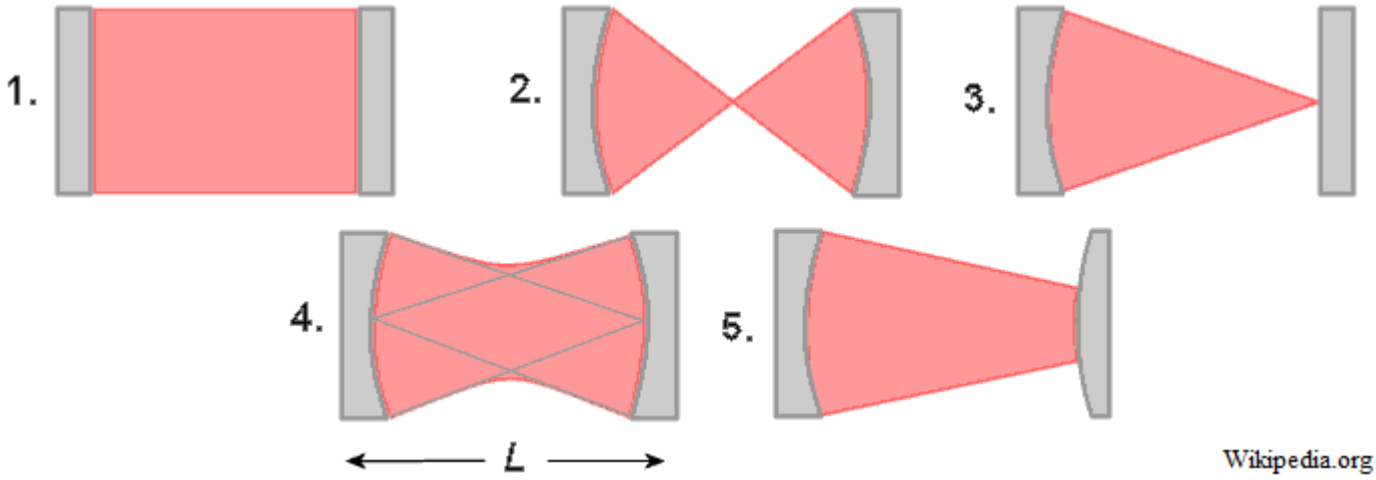

Figure 4: Schema of different kind of cavities. 1. plan-plan cavity, 2. concentric cavity, 3. plan-concave cavity, 4. confocal cavity, 5. convex-concave cavity

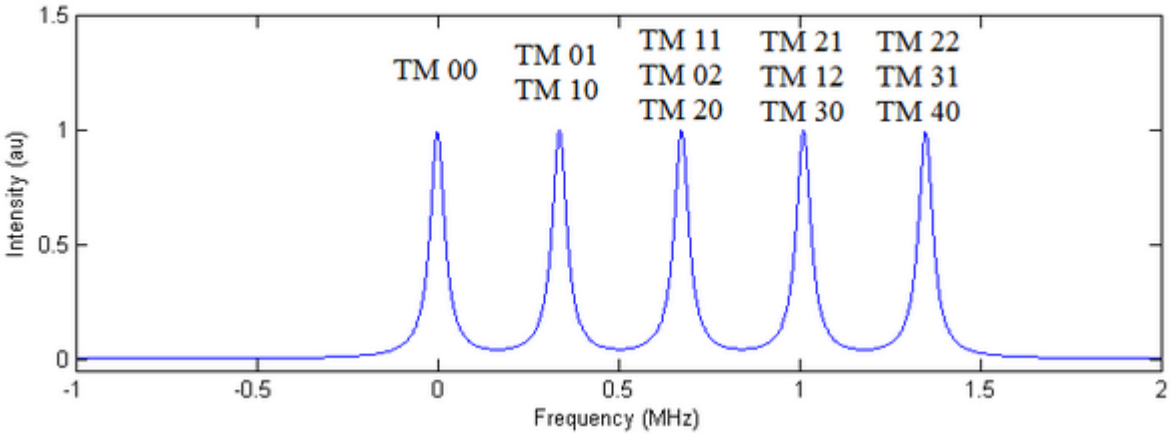

Figure 5: Simulation of a near concentric cavity. R_1=R_2=0,5 m and L=0.99995 m. Computed with FINESSE.

In a fully degenerate cavity we should find only one resonating peak in a FSR. The FSR is defined as the difference of frequency between two consecutive longitudinal modes of the same transversal mode, FSR= ν_{q+1,n_0,m_0}- ν_{q,n_0,m_0}= $\frac{c}{2L}$. In other words the difference of frequency between every modes should be 0 or an integer multiple of the FSR.

According to the Eq. 1 we can fulfill the condition of degeneracy if $\frac{cos^{-1}(\pm\sqrt{g_1 g_2})}{\pi} \in \mathbb{Z}$. There is also a condition on g_1 and g_2. For a stable cavity$0 \leq g_1 g_2 \leq 1$. Two solutions are available : $\frac{cos^{-1}(\pm\sqrt{g_1 g_2})}{\pi} = 0$ or 1. These solutions correspond , respectively, to a plane-plane cavity and a concentric cavity (see fig.2.1). In practice these cavities are not good choices in our case. They are too close to instability, particularly the plan-plan cavity. In this cavity, the size of the beam only grows. Quickly the beam will become bigger than mirrors introducing lot of losses.

The other solution is to use a half degenerate cavity, if $\frac{cos^{-1}(\pm\sqrt{g_1 g_2})}{\pi} = \frac{1}{2}$ then even and odd modes will resonate at different frequencies. But all odd modes will resonate

at the same frequency. Same thing for even modes. Odd modes will resonate at half FSR from even modes, it means every $\frac{FSR}{2}$ we can see a peak of transmission. We can reach this condition with a confocal cavity. Furthermore, with a confocal cavity we do not have any instability problems (see fig. 6).

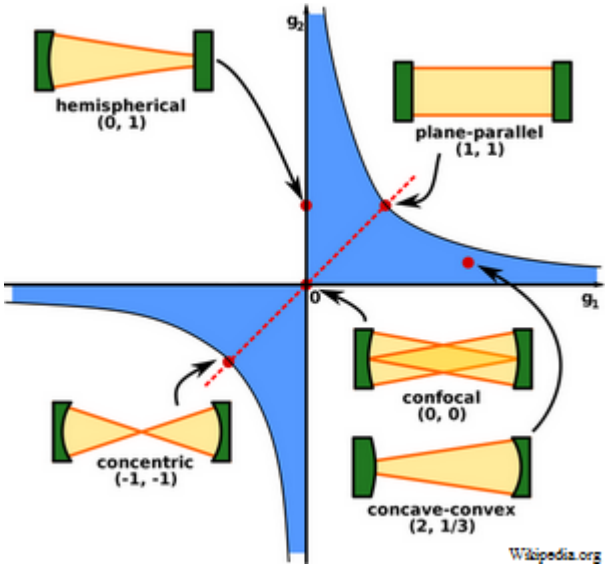

Figure 6: Diagram of stability for 2 mirrors cavities in function of g_1 and g_2. Blue areas are stable areas.

On the contrary of plane-plane and concentric cavities if we change the length of a confocal cavity, the working point will move along the dash red line and stay in stable areas.
The drawback of using a half degenerate cavity instead of a fully degenerate ones is the operating frequency range is divided by 2. Let's take a fully degenerate cavity with a FSR of 300 MHz. If we modulate the beam at a frequency of 100 MHz then we scan the cavity, we will see a carrier, a sideband at 100 MHz from the carrier, an other sideband at 200MHz and an other carrier at 300 MHz. In this case there is no problem, the first sideband is the upper sideband of the first carrier and the second sideband is the lower sideband of the second carrier (see fig. 7 (a)).

Now if we do the same with a half degenerate cavity we will find a sideband at 50 MHz from the first carrier, a sideband at 100 MHz and a other carrier at 150 MHz. The first sideband is the lower sideband of the second carrier and the second sideband is the upper sideband of the the first carrier. Even and odd modes sidebands are mixed (see fig. 7 (b)).

With only one modulation it is not difficult to identify sidebands but when there are 4 modulations then it becomes difficult. In the cavity design we have to take care about this. In order to not mix up even and odd sidebands, we need to fulfill this condition: MF (Modulation Frequency) $<$ FSR/4 for a confocal cavity. The highest modulation frequency we have to resolve is 56.4 MHz, it means we need a FSR bigger than 225.6 MHz.

We want to extract the sidebands amplitude in order to control the symmetry of the interferometer. It means that the sidebands must be far enough away from the carrier to neglect the amplitude of the carrier in front of the amplitude of the sideband. Considering that the closest RF sideband from the carrier is 6.27 MHz and we want less than 0.1 % of the amplitude of the carrier we need a FWHM of 390 kHz. The finesse of the cavity, $F = \frac{FSR}{FWHM} = \frac{\pi(R_1R_2)^{1/4}}{1-\sqrt{R_1R_2}}$, should be at least equal to 600. To reach a finesse of 600, we need mirrors with a reflectivity of 99.5 %.

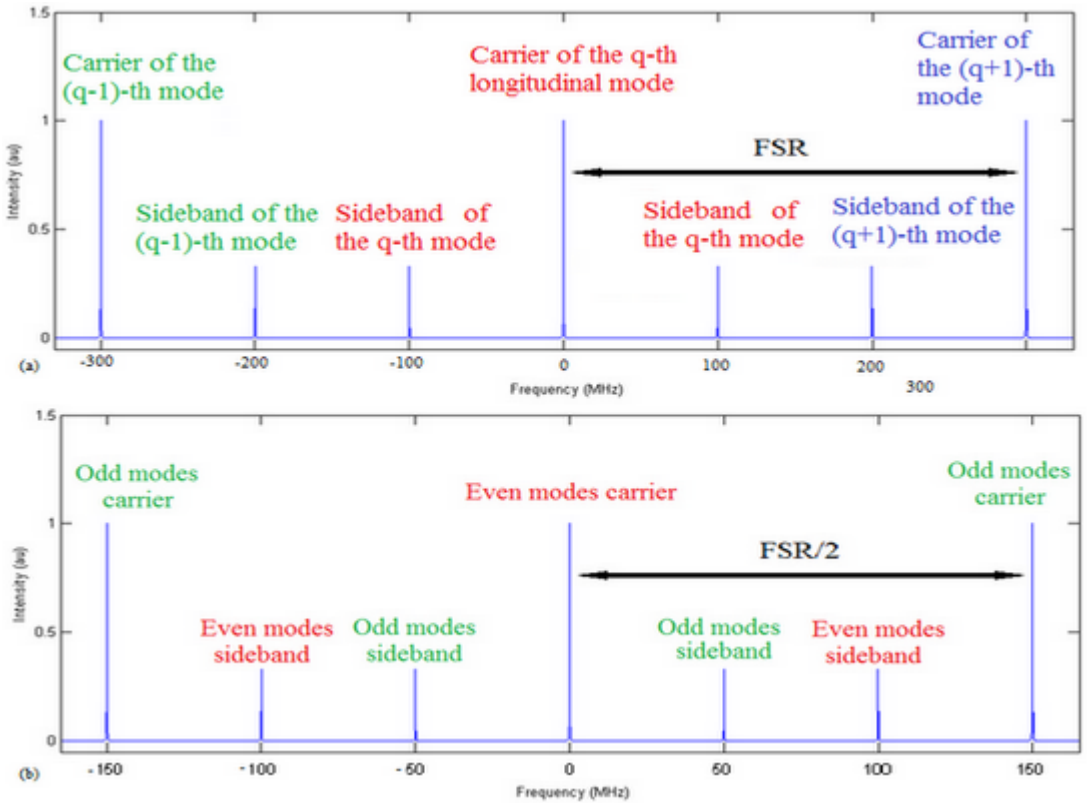

Figure 7: Simulation of a confocal cavity with a FSR of 300 MHz and RF modulation at 100 MHz. Computed with FINESSE.

The cavity has its own eigenmodes, if we send any kind of beam inside the cavity the transmission will be weak. Because the coupling between cavity and beam is weak. To improve the coupling we need to match the beam to the cavity. Mode-matching consists in mold the laser beam into the cavity resonating modes. Fortunately the laser beam and the cavity modes are both gaussian [7]. First we need to calculate the size and the position of the waist of the cavity. Considering the symmetry of the cavity, the waist can only be in the middle of the cavity. The size of the waist in a symmetric cavity is given by :

$$w_0 = \sqrt{\frac{\lambda L}{2\pi}\left(2\frac{|R|}{L} - 1\right)^{1/2}} \tag{2}$$

with L the length of the cavity, λ the wavelength of the laser and R mirrors radius of curvature. It is also interesting to know the waist size on each mirror. We can easily know the size of the beam on mirror by propagating a gaussian beam The beam must be smaller than mirrors or the finesse of the cavity will decrease because of losses

Beam characteristics are usually given by the laser manufacturer, then it is easy to design a telescope with an ABCD matrix algorithm to match the beam with the cavity. The mode-matching can be done in general with one lens, but most of the time the focal length will not be common. It is more convenient to use a couple of lens.

In order to complete our goal, we need a cavity with a FSR of 225.6 MHz and a FWHM of 390 kHz.

2.2 Alignment and characterization of the SFP

Before starting the alignment of the SFP cavity, we need to know the approximative position of all components. The most critical part is the position of the telescope and the cavity.

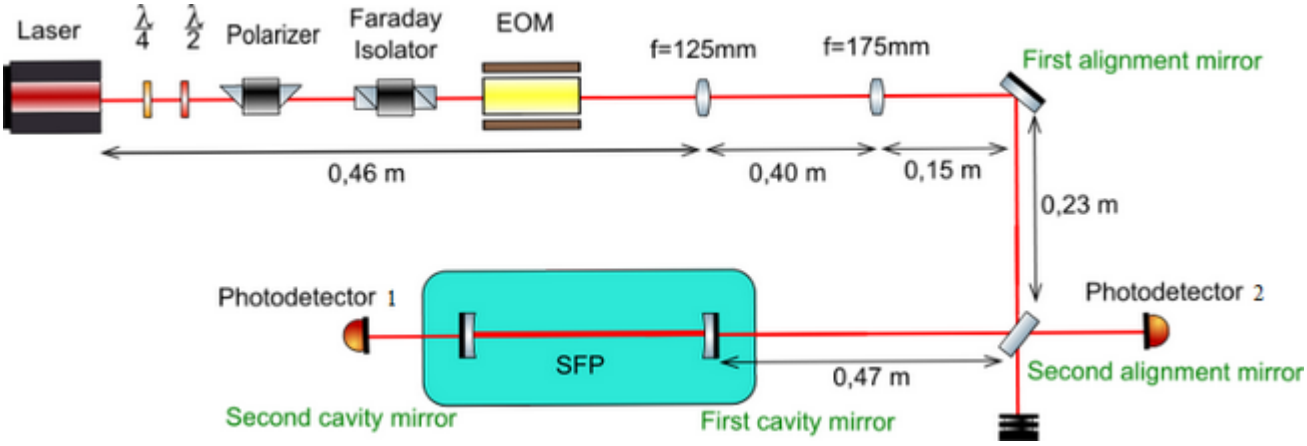

Figure 8: Schema of the setup.

	SFP parameters
Length	0,5 m
FSR	300 MHz
Finesse	> 1500
Waist raduis	290 µm
Output/input mode radius	410 µm
FWHM	< 200 kHz

Figure 9: Table of relevant parameters of the SFP cavity.

Polarizer, λ /2 and λ /4 plates are used to decrease the laser power. Faraday isolator avoid light feedback in the laser which can disturb the smooth working of the laser. We modulate the beam with an electro-optic modulator (EOM) then we can use sidebands as a frequency scale for measurement. Lenses are here for the mode-matching, it is better to put the telescope before alignment mirrors. In this way, when we align the beam in the cavity we do not change the alignment of lenses.

Mirrors with a radius of curvature 0.5 m and a reflectivity of 99.8 % have been purchased in order to build a cavity. We can see in fig. 9 parameters of the confocal cavity built with these mirrors. These specifications agree with our requirement.

2.2.1 Mode matching

First, we measured the size of the beam at different distances from the laser in order to characterize the waist and the position of the waist. If we measure the size of the beam at different position from the laser we can use the divergence of the beam and the wavelength to know the waist and the position of the waist. The beam radius in function of the distance from the waist is given by:

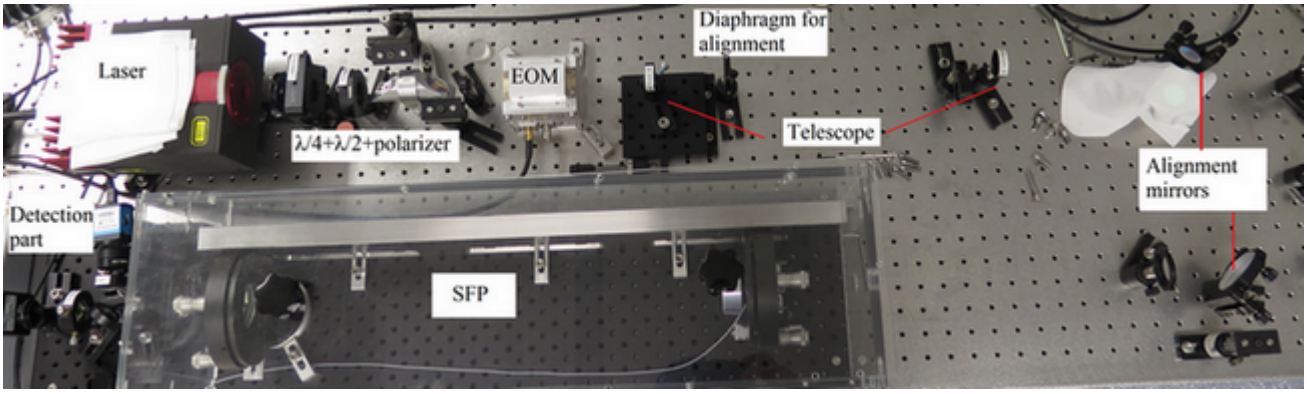

Figure 10: Picture of the setup.

$$\omega(z) = \omega_0 \sqrt{1 + \left(\frac{z}{z_0}\right)^2} \tag{3}$$

with ω_0, the waist of the beam and z_0, the Rayleigh parameter.

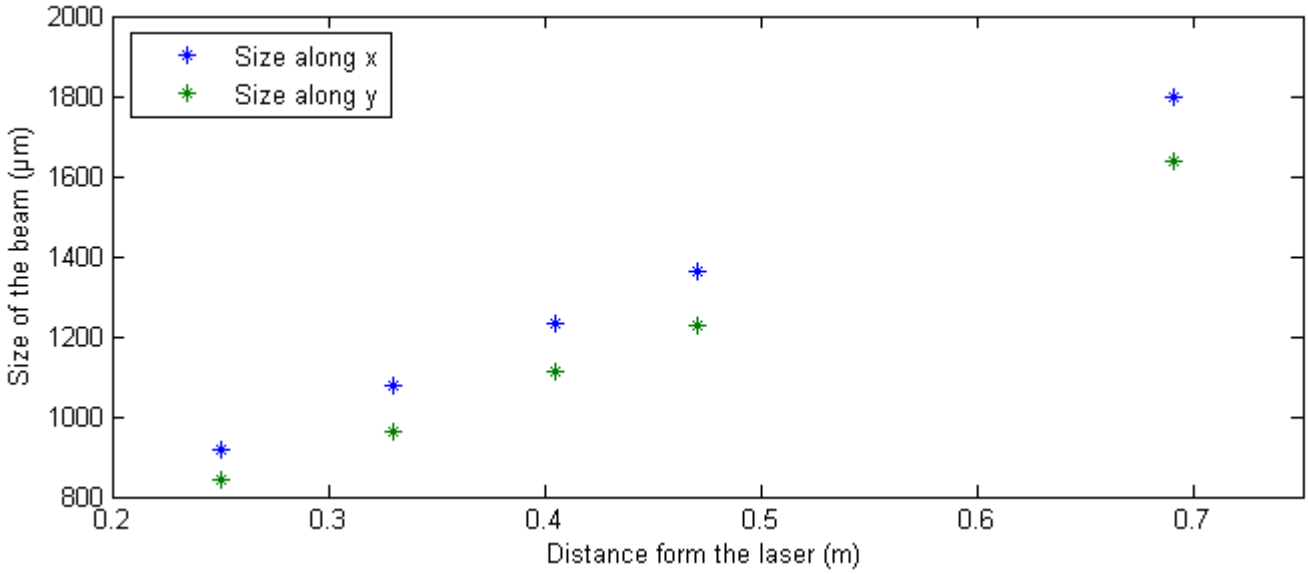

Figure 11: Size of the beam in function of the distance from the laser.

We can see, in fig. 11, that the beam is a bit astigmatic. We have found that the waist along x and y are respectively 170±15 µm and 188±17 µm. According to the constructor the position of the waist is around 105 mm inside the head of the laser. Now we know the position, the waist of the beam and the waist of the cavity, we can design a telescope to mode-match the beam on the cavity (see fig. 12). We used a ABDC matrix algorithm to find a waist close to the cavity waist and in an available position in the setup (see fig. 8 and 10).

We also characterized the beam after the telescope. (See fig. 13) The beam is still astigmatic, it could worsen the mode-matching on the cavity. Waists along x and y are respectively 255±21 µm and 224±10 µm. Waists in x and y are not at the same position,respectively at 0,1 cm and 6 cm, this is also bad for the matching.

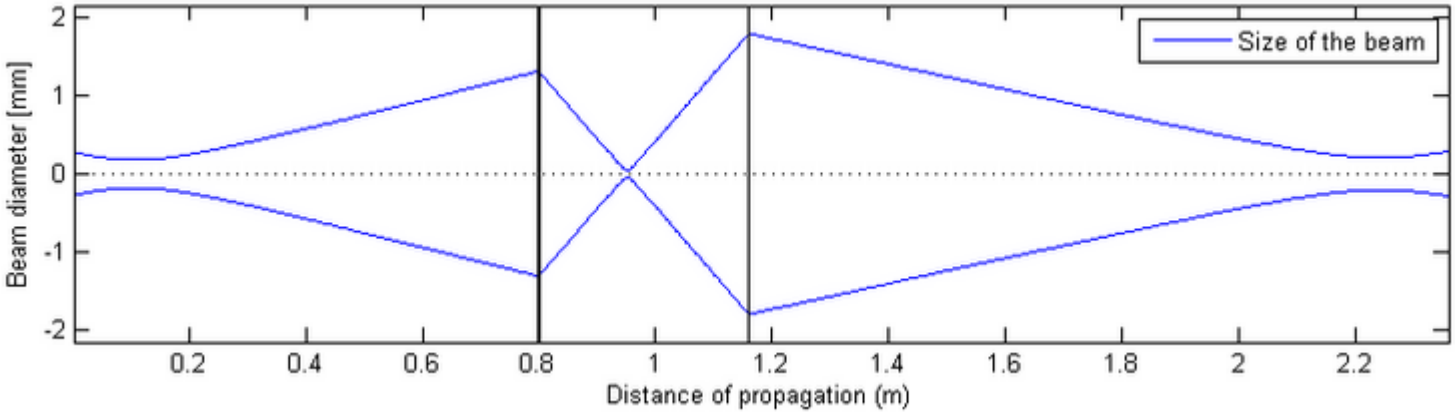

Figure 12: Propagation of the beam through the telescope.

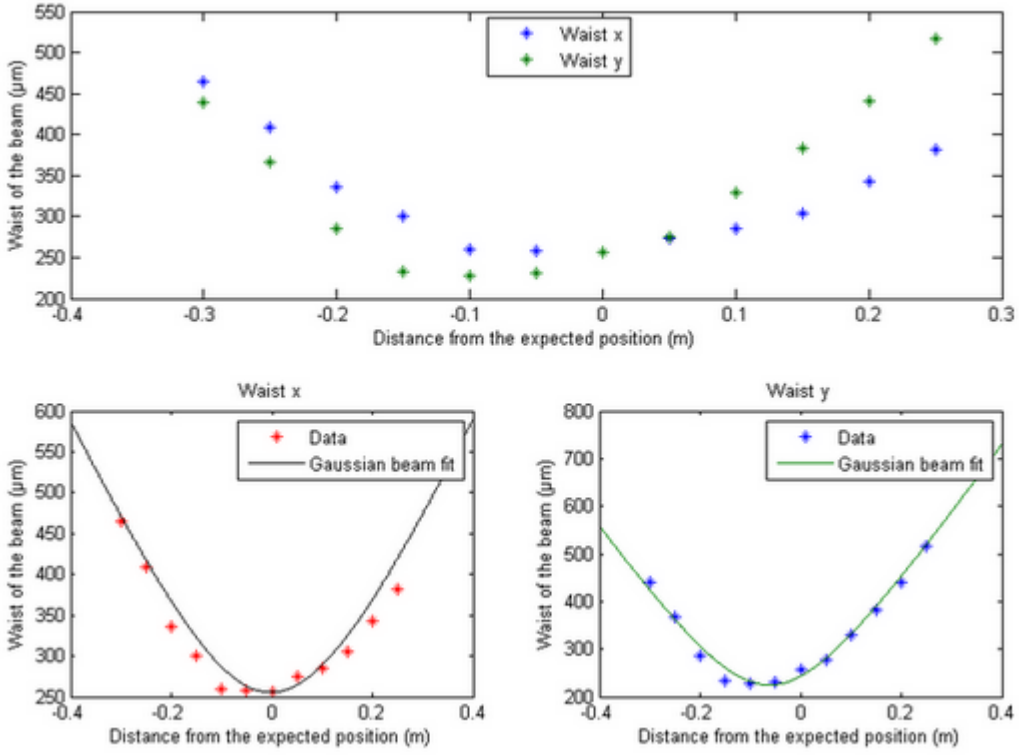

Figure 13: Size of the beam after the telescope.

The coupling between the fundamental mode of a cavity and an astigmatic TM_{00} beam is given by: [8]

$$|\Gamma|^2 = \frac{4w_0^2 W_x W_y}{\sqrt{(w_0^2 + W_x^2) + \frac{b^2 W_x^4}{R_x^2}}\sqrt{(w_0^2 + W_y^2) + \frac{b^2 W_y^4}{R_2^2}}} \tag{4}$$

with w_0, the waist of the cavity,w_n, the waist along x or y,L_n, the distance from the waist considered and b_n, the Rayleigh parameter along x or y.

$$b_n = \pi w_n^2/\lambda \qquad W_n = w_n\sqrt{1+\frac{L_n^2}{b_n^2}} \qquad R_n = L\left(1+\frac{b_n^2}{L_n^2}\right)$$

Even if conditions are not the best, the coupled power into the cavity is still reasonably good. In this condition we can expect a coupling of 86 % (see fig. 14) of the incoming power on the fundamental mode of the cavity. In practice this rate will never reach because of imperfections. The coupling is not very sensitive to a longitudinal translation of he cavity, we only lose 3% of coupled power if we place the cavity at 5 cm from the most efficient position.

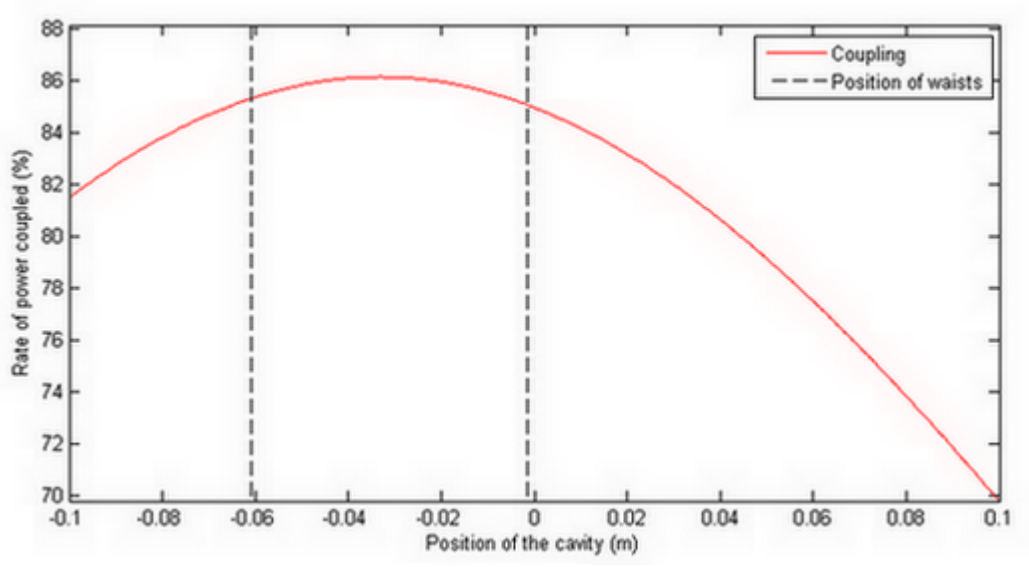

Figure 14: Coupling between the beam and the cavity in function of the position of the cavity.

The mode-matching is not only useful to increase the coupled power, it also help during the alignment of the cavity. If the matching is not well done then we couple lot of modes into the cavity (see fig. 15). The accuracy on the length of the cavity needed to merge all modes increase when there are lot of modes [9].

In fig. 15 (a), we can see most of the power is coupled into few modes and particularly into the fundamental mode. With a bad mode-matching, lot of modes resonate in the cavity. In fig. 15 (b) ,there are more than 30 modes resonating in the cavity. When the coupling is efficient we can see easily if we look at are odd or even modes but when these is lot of modes, we can't say anything. We only see half of modes in fig. 15, there is the same profile for the others modes. The beam alignment into the cavity is very important for the mode-matching.

2.2.2 Alignment of the beam on the optical axis

To align the beam we need a mirror and a target (see fig. 8 and fig. 10). The target must be stable and we need to be able to move it and be sure we can put it back in

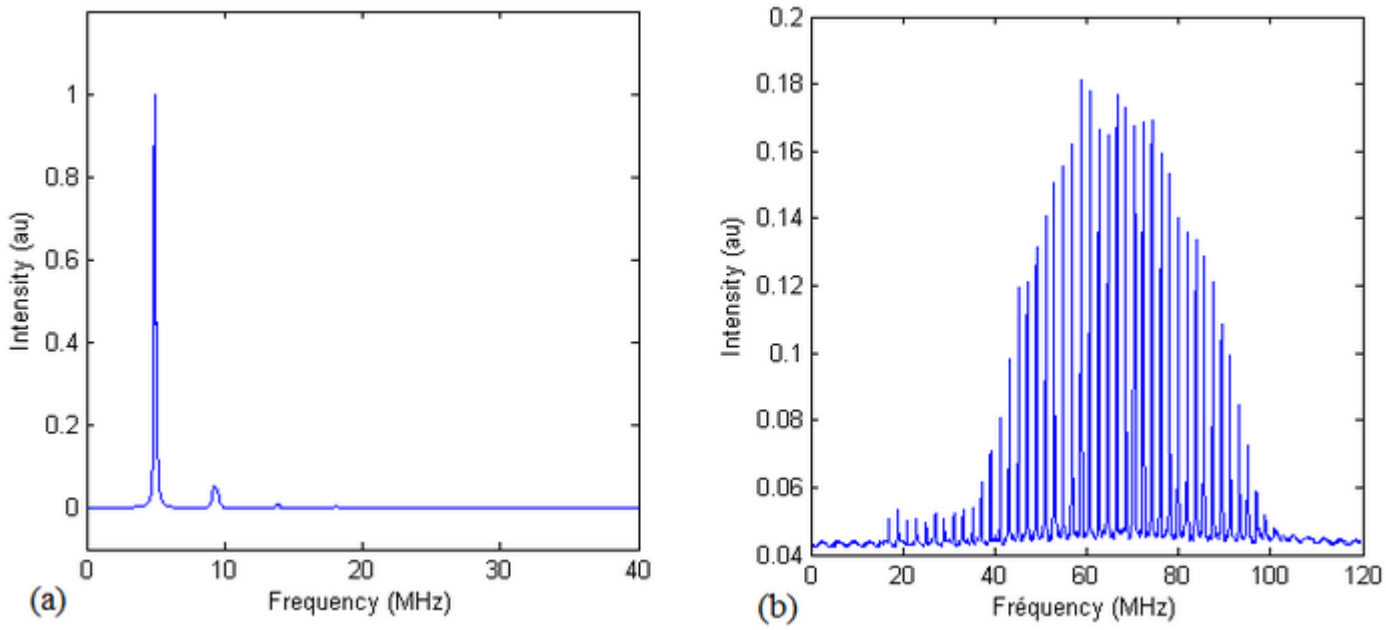

Figure 15: Transmitted power through a near confocal cavity. (a) with good mode-matching, (b) with bad mode-matching.

the same previous position. To be sure to align the beam in the middle of mirrors, we used a special target.

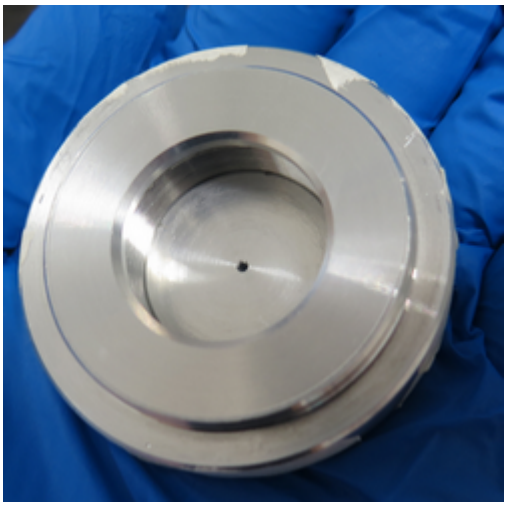

Figure 16: Target used for the alignment of the beam.

We design a piece made aluminum that we can put into the mounts that will be used to hold the mirrors of the SFP cavity. We also design supports for mirrors which be mounted on the piezoelectric actuator and 1 inch adapter (see annexes A, B,C, D and E). The target consists in a piece of aluminum of 2 inch diameter with a hole of 1 mm in the middle. Then, we used a power meter and maximize the transmission into the hole.
The beam alignment is done in two steps, first we align the beam on the target (called Target 1) close to the second alignment mirror. This target will be sensitive to shift from the optical axis. Then, we align on the target (called Target 2) far from the second alignment mirror.

This target will be sensitive to tilt from the optical axis. Using one alignment mirror and Target 1, we align the beam on the target. Then we do the same thing using Target 2 but we must use the other mirror alignment (see fig.17). We should use targets and alignment mirrors in pairs. For example, we always use the first mirror to align the beam on Target 1 and the second one to align on the Target 2.

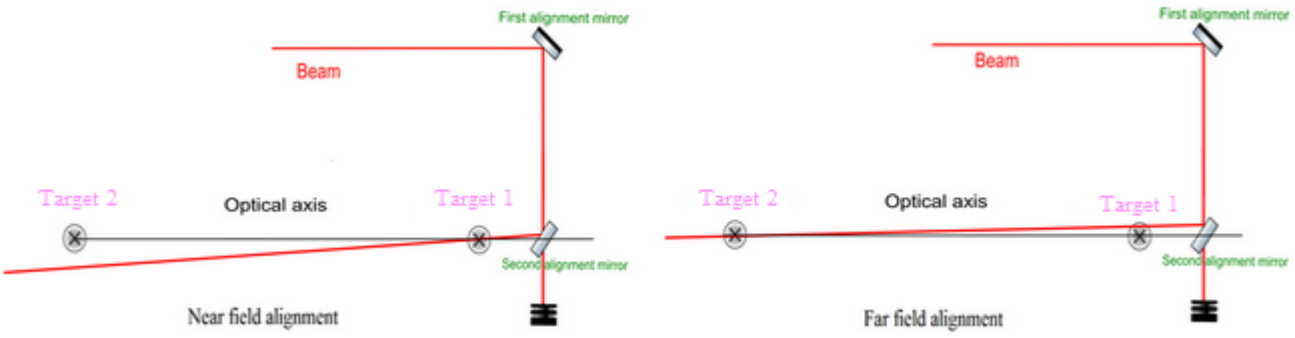

Figure 17: Schema of the two steps for the alignment of the beam along the optical axis of the cavity.

We have to repeat these two steps until the beam stay in the middle of the target regardless the position along the optical axis as show in fig. 18 Further is the target 2 and closer is the target 1 better is the alignment. At this point, we should not touch alignment mirrors anymore.

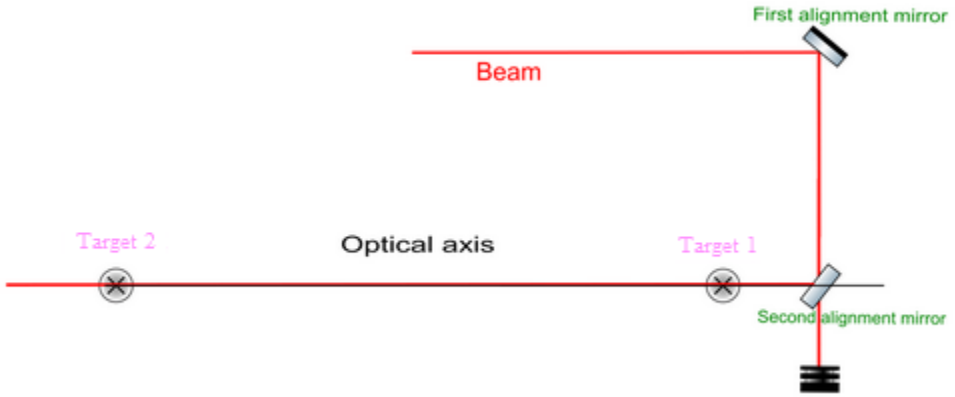

Figure 18: Schema of the aligned beam.

Before putting mirrors in mounts, we need to align the detection part. It is easier to do it now because the beam is easy to find. After we place mirrors the transmission will be weak so it is difficult to see the beam. It is a good idea to use a camera to see the shape of the transmitted beam, it will help to keep the alignment of cavity mirrors. We also use a photo diode Furthermore the beam is not deflected by the cavity when the cavity is aligned.

2.2.3 Alignment of the mirrors of the cavity

Now we need to align the orientation of mirrors of the cavity. The reflected beam must coincide with the incident beam. We used a diaphragm at the beginning of the setup (see fig.10), further is the diaphragm from the cavity better the alignment of the mirror will be. We can also use a beam splitter as a alignment mirror, in this case we can access the reflected beam and use a power meter to improve the alignment as showed in fig. 19

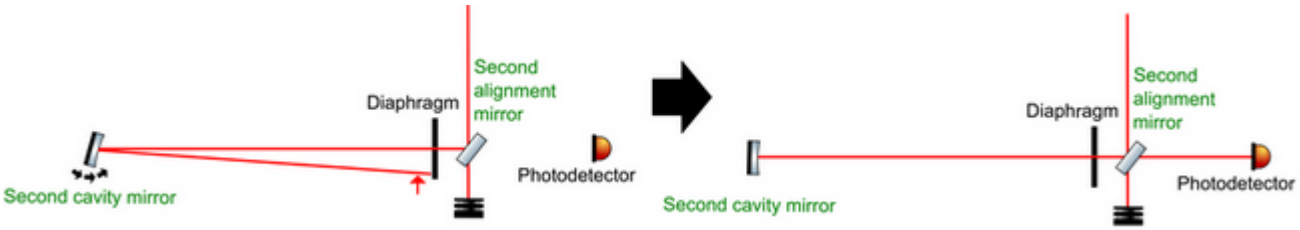

Figure 19: Schema for the orientation of mirrors.

We must start the alignment this the second cavity mirror. When the second cavity mirror is align, we do the same with the first cavity mirror. At this point if we start scanning the SFP cavity we should see light in transmission of the cavity.

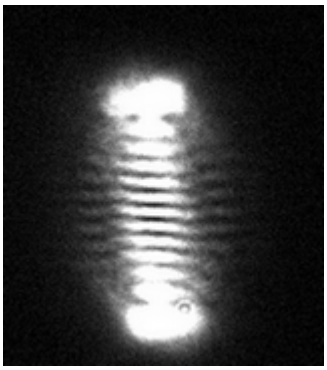

Figure 20: Shape of the transimitted beam with a misalignment of mirrors of the cavity.

Using the camera we can adjust precisely the align of mirrors. If modes look likes the fig. 20 it means that there is a misalignment in the vertical way. In this case we have to tilt one mirror and compensate with the other until the transmitted mode becomes circular (see fig.21). If the cavity is well align we should be able to tell which peaks are odd modes and which one are even modes. It is useful to keep the camera all along the alignment procedure, specially during adjusting of the length of the cavity. The translation stage will introduce some misalignment so we need to check and compensate, if needed, every time the alignment of mirrors. The next step is the adjustment of the length of the cavity.

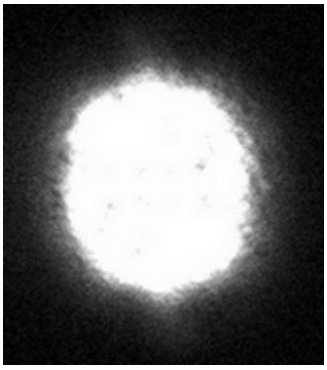

Figure 21: Shape of the transimitted beam with a good alignment of mirrors of the cavity.

When the cavity is not in its confocal configuration, we can see all modes resonating at different frequencies. But when we go closer to the confocal point, all peaks merge and we see only one peak. If we are close enough from the confocal point and when peaks are close enough from each other then we cannot distinguish modes. As a result we see a peak which looks like lorentzian but the FWHM is bigger (see fig. 22). This effect is more important when there are lots of modes into the cavity. But we can use the finesse to know if the length cavity is good enough. The finesse is independent of the length of the cavity and can be measured experimentally with the FSR and the FWHM. If we measure the finesse when modes are all separated then we can measure the finesse of the cavity (see fig.23).

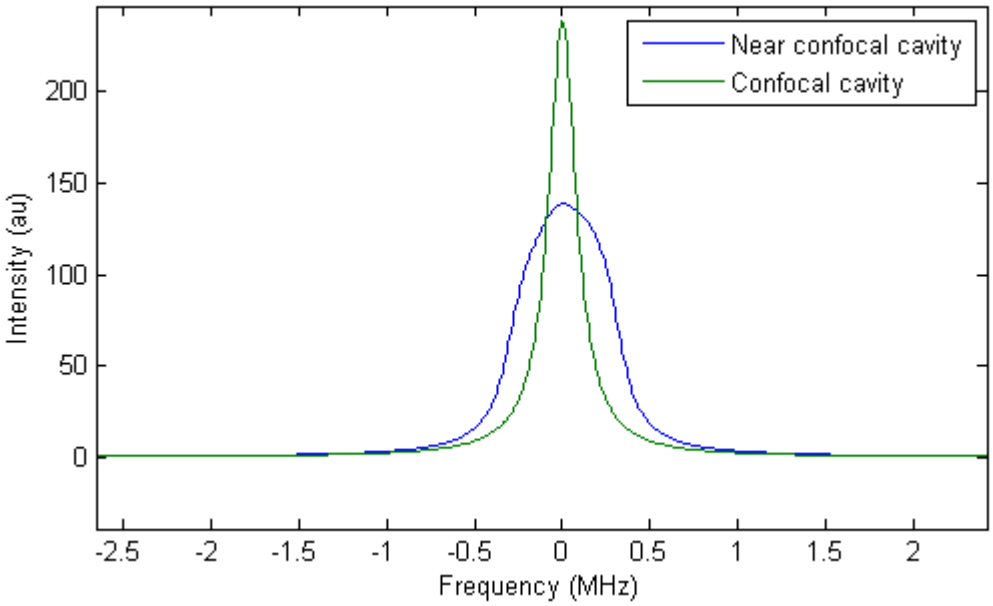

Figure 22: Simulation of a cavity with a finesse of 1500, a FSR of 300 MHz and 15 modes resonating. There is 100 µm mistake on the length of the near confocal cavity. Computed with FINESSE.

With the data in fig. 23, we found a finesse of 1830. We can compare this finesse with the one we will measure and the length of cavity will be adjusted, then we can know how good is the adjustment of the length.

2.2.4 Adjustment of the length of the cavity

The adjustment of the length of the cavity is critical on the resolution. We start far from the confocal point, using an oscilloscope we look at the shape of the peaks in transmission. When we come closer to the confocal point peaks merge, then it become difficult to see if we improve or worsen the adjustment. We used a translation

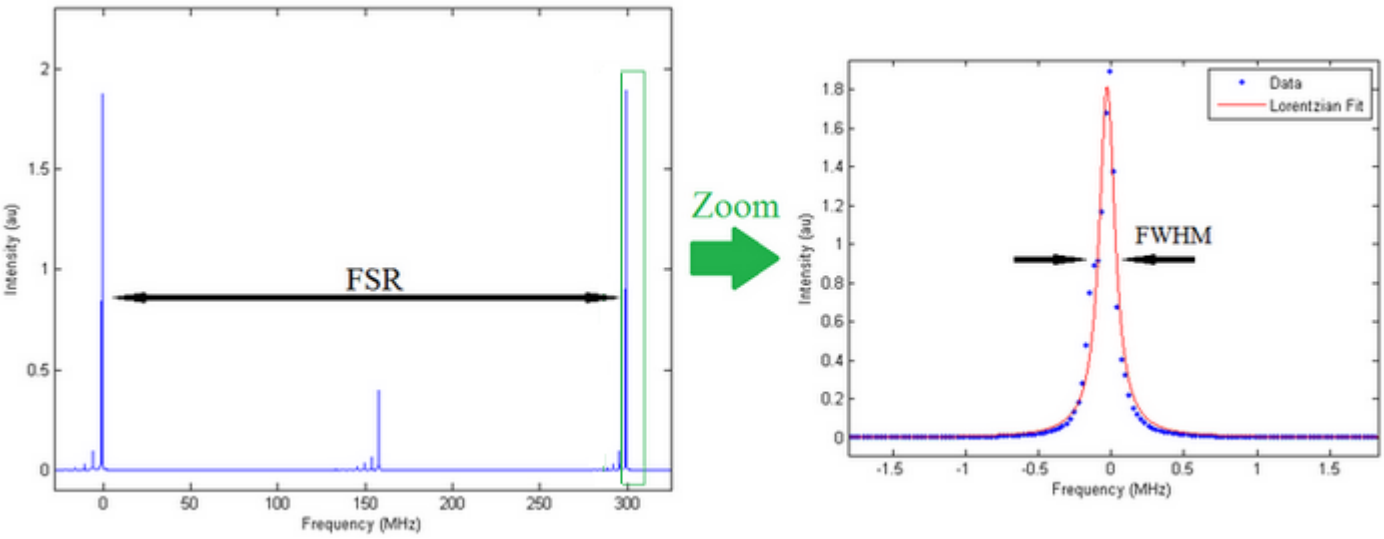

Figure 23: Measurement of the finesse of the cavity when all modes are separated. We use a lorentzian model to fit the data in order to extract the FWHM.

stage with an accuracy of 10 µm. We moved the mirror step by step and we recorded data at every step. Then we measure the finesse of the cavity and we compare it with the finesse measured when the cavity was far from the confocal point. In theory we should find the same finesse when the length of the cavity is perfectly adjusted but, in practice it never happen.

On the contrary to the simulation in fig. 22 where all modes had the same amplitude and when there is few modes, we can see an asymmetry on the shape of the transmitted peak (see fig. 24).

Also something interesting is that the asymmetry changes if we cross the confocal point. We can use this property to determine the position of the confocal point.

2.2.5 Stabilization of the cavity

The cavity is very sensitive to external perturbation like air turbulences or mechanical vibrations. So we need to isolate the cavity from these perturbations. To avoid air turbulences inside the cavity, we design a box in plexiglas (see Annex F). We decide to do not fixed the box on the breadboard in order to avoid mechanical stress (see Annex G). To limit the effect of mechanical vibrations on the cavity, we designed a plate in steel and we screwed the mounts of the cavity on the plate.

The stabilization of the cavity is efficient for small perturbation.

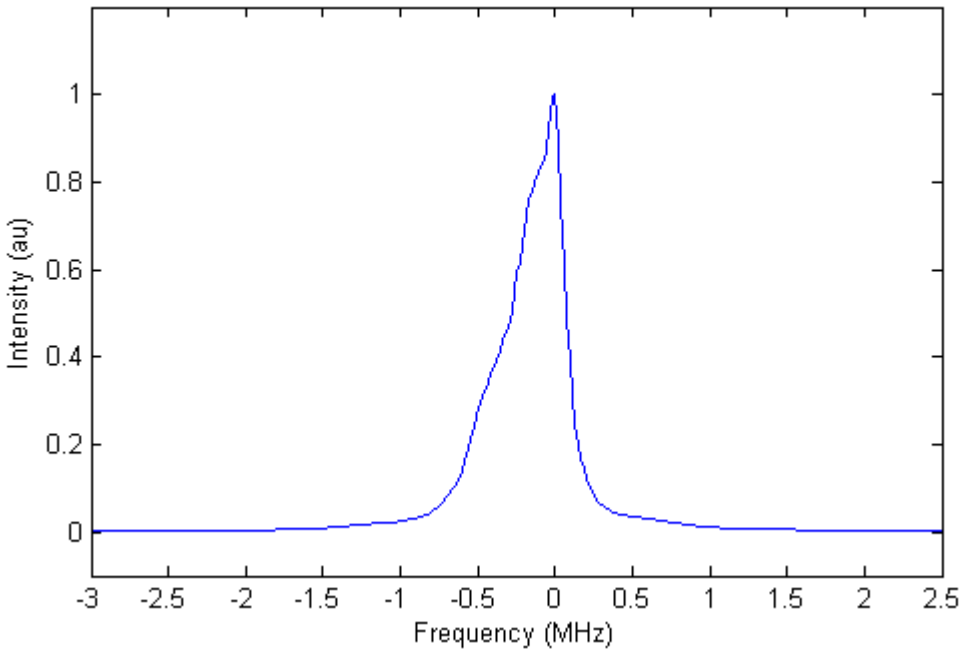

Figure 24: A near confocal cavity. We can guess higher modes on the left part of the peak.

In fig. 25 (b) and (c) we can see sidebands, but on fig. 25 (a) there is no modulation.

2.3 Experimental results

To determine the resolution of the cavity, I measured the FWHM on 15 different peaks and the FSR.

FWHM (kHz)			FSR (MHz)
200.47	150.96	191.59	297.70
150.48	172.36	162.50	297.57
207.93	160.10	158.17	288.46
152.40	136.54	179.09	297.50
196.89	190.87	181.03	288.78

Table 1: Table of raw data used to determine the resolution of the cavity.

Using the data in table 1, we found these parameters:

$$FWHM = 172.76 \pm 21.64\ kHz$$

$$FSR = 293.07 \pm 4.96\ MHz$$

We can compute the finesse of the cavity to know how well the cavity is aligned.

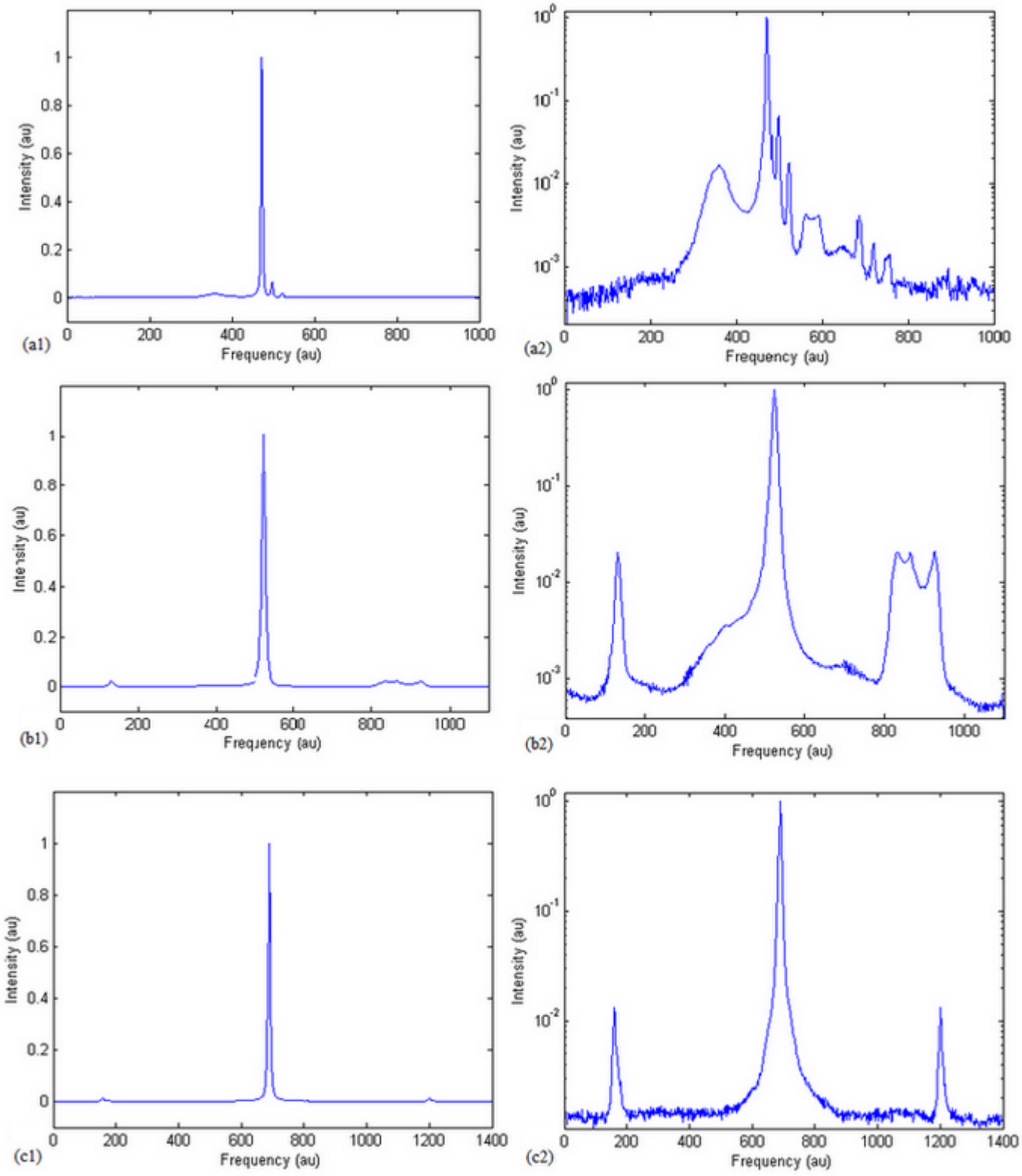

Figure 25: Shape of a transmitted peak in linear and logarithmic scale. (a) without box without plate, (b) with box without plate, (c) with box with plate.

$$F = 1696.5 \pm 28.69$$

The finesse of the aligned cavity is close from the finesse computed with the fig. 23, it means the length of the cavity is good.

	SFP parameters	Coherent parameter
Length	0,5 m	0.25 m
FSR	300 MHz	600 MHz
Finesse	> 1500	> 400
Waist raduis	290 µm	205 µm
Output/input mode radius	410 µm	290 µm
FWHM	< 200 kHz	< 1.5 MHz

Figure 26: Comparison of the parameter between the SFP and the commercial coherent cavity used on VIRGO.

With the new cavity, we can expect a resolution 8 times better than with the Coherent cavity (see fig. 26). The Coherent is not able to resolve clearly the 6.27 MHz modulation sidebands (see fig. 27). On the blue curve, we can see sidebands at 6 and 22 MHz, 6 MHz sidebands are in the tail of the carrier. Even 22 MHz modulation sidebands are not clearly out of the tail of the carrier. On the green curve, we can see sidebands at 12.25 MHz. Sidebands are clearly out of the tail of the carrier. The new SFP should be able to resolve the 6 MHz modulation sidebands.

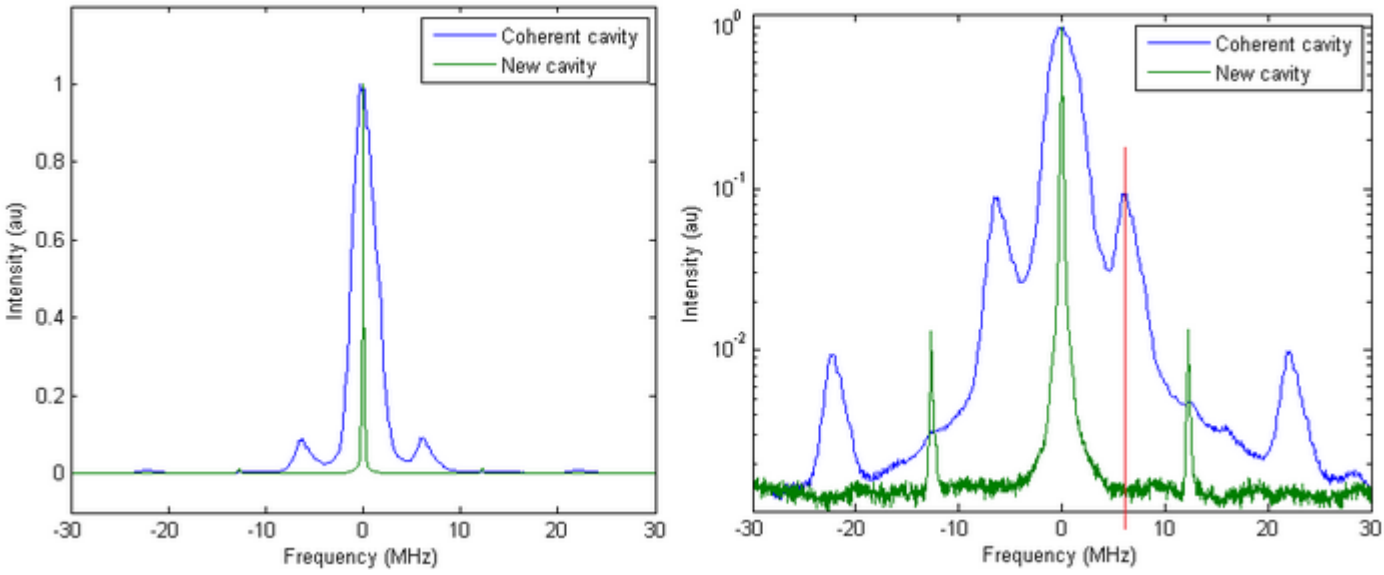

Figure 27: Comparison between the new SFP and the commercial coherent cavity used on VIRGO in linear and logarithmic scale.

3 Scanning Fabry Perot Imager (SFPI)

3.1 Theoretical part

On the contrary of the confocal cavities, SFPI cavities are completely degenerate. All modes (even and odd) resonate at the same frequency. That is why we called it Imager, if all modes resonate at the same frequency then the transmitted beam should have the same shape than the incident beam. Such a cavity has been described by [10] and [11]. From a geometrical point of view any optical ray come back on itself after a round trip (see fig.28).

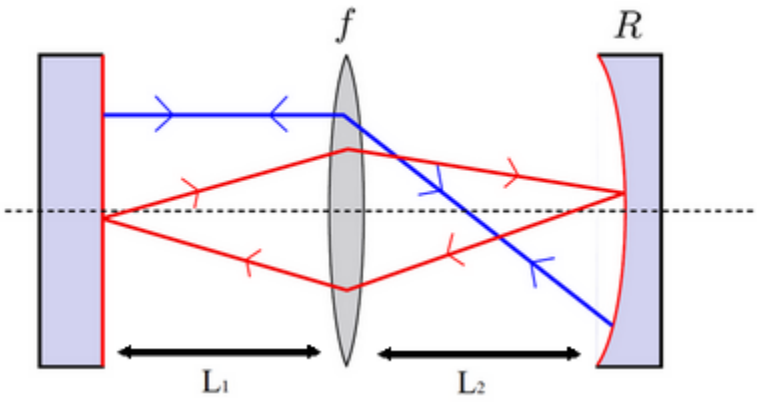

Figure 28: Schema of a fully degenerate cavity.

The ABCD matrix of such a cavity is identity:

$$\begin{pmatrix} A & B \\ C & D \end{pmatrix}_{cav} = \begin{pmatrix} 1 & 0 \\ 0 & 1 \end{pmatrix} \tag{5}$$

Also mode-matching does not matter, this cavity has not any eigenmodes. Eigenmodes are mode which can resonate into the cavity. Let consider a mode defined by a q-parameter, $\frac{1}{q(z)} = \frac{1}{R(z)} + i\frac{\lambda}{piW^2(z)}$ with R(z), the radius of curvature, λ, the wavelength, W, the half size of the beam and z, the distance of propagation from the waist of the beam. We can compute the propagation of a guassian beam trough an optical system used ABCD matrix. The q-parameter after an optical system is given by the ABCD law:

$$q_2 = \frac{Aq_1 + B}{Cq_1 + D} \tag{6}$$

An eigenmodes is mode a which still the same after a round trip into the cavity. It must satisfy the fallowing condition :

$$q_{cav} = \frac{Aq_{cav} + B}{Cq_{cav} + D} \tag{7}$$

In our case A=D=1 and B=C=0. It means every gaussian beam satisfies the condition 7. The cavity do not have any eigenmode or all gaussian solutions are

eigenmodes of the cavity. The main limitation is the size of optical elements (numerical aperture) and the accuracy with which optical elements are aligned.

The cavity described in fig. 28 consisting of a plane mirror, a lens of focal length f an a spherical mirror of radius of curvature R. For a fully degenerate state the length L_1 and L_2 must satisfy these conditions:

$$L_{deg1} = f + \frac{f^2}{R} \tag{8}$$

$$L_{deg2} = f + R \tag{9}$$

The fully degenerate state is only reach when L_1=L_{deg1} and L_2=L_{deg2}. If the cavity is not fully degenerate when it has eigenmodes. In this case if we scan the cavity, we will see all modes resonating at difference frequencies.

3.2 Alignment procedure and characterization of the SFPI

The setup for this cavity is the same than the SFP one. Mirror with a radius of curvature of 0.1 m, 0.075 m and plane mirrors with a reflectivity of 99.5% have been purchased in order to build a cavity. We also design a box and a plate for the stabilization of the cavity (see Annex H and I).

Some steps of the alignment procedure are the same for both cavities.

The procedure to align the beam on the optical axis of the cavity is the same for the SFPI than SFP.

The main difference between the SFP and the SFPI is the lens. We need to align the lens before the mirrors. We assumed that the beam is align on the optical axis of the cavity. The lens should not deflect the beam from the optical axis. If the lens is well aligned then the beam will stay in the middle of the Target 2. In this case we are sure that the beam is in the middle of the lens. We used the lens with a translation mount to align precisely the lens.

The alignment of the mirrors of the cavity is done in the same way than the SFP. The SFPI is very sensitive to the alignment of the mirrors, we need to do it very carefully. A camera is useful for the alignment of the mirrors and the adjustment of the lengths

We use the instable area to adjust both lengths. With the camera, we can see when we go in instable area. The radius of the transmitted beam suddenly increase and the transmitted power decrease.

First we need to start far from the degenerate stat but not in a unstable area. In our case, we started with the concave mirror further from the lens than the degenerate length L_{deg2} and the plane close from the lens than the degenerate length L_{deg1} (see fig. 29). We move the concave mirror closer to the lens until we meet the unstable area. Then we move a bit the plane mirror further from the lens. We have to repeat these two steps until we reach the fully degenerate state.

Step by step we will see that the transmitted power increases and all modes starts merging (see fig.30). During the adjustment of the lengths, we have to check the alignment of the mirrors with the camera. The translation stage will introduce some misalignment and we need to compensate it at every steps.

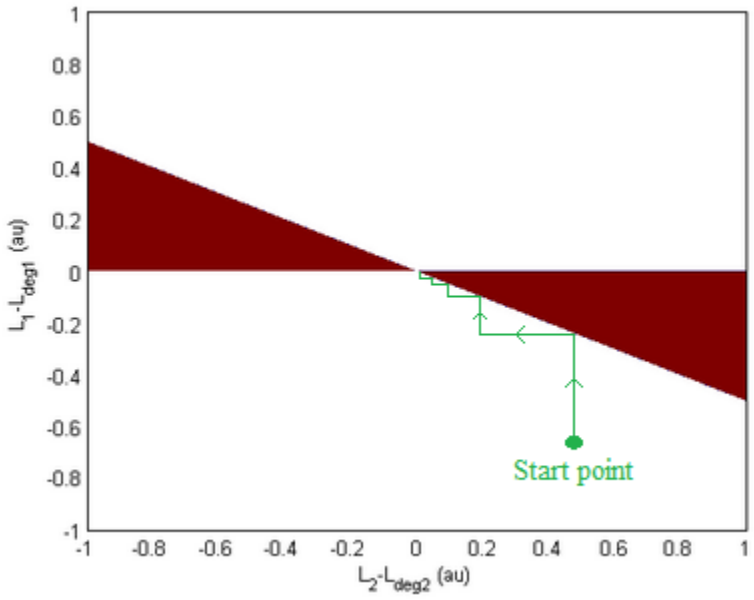

Figure 29: Adjustment procedure of the lengths of the SFPI. Red areas are unstable areas.

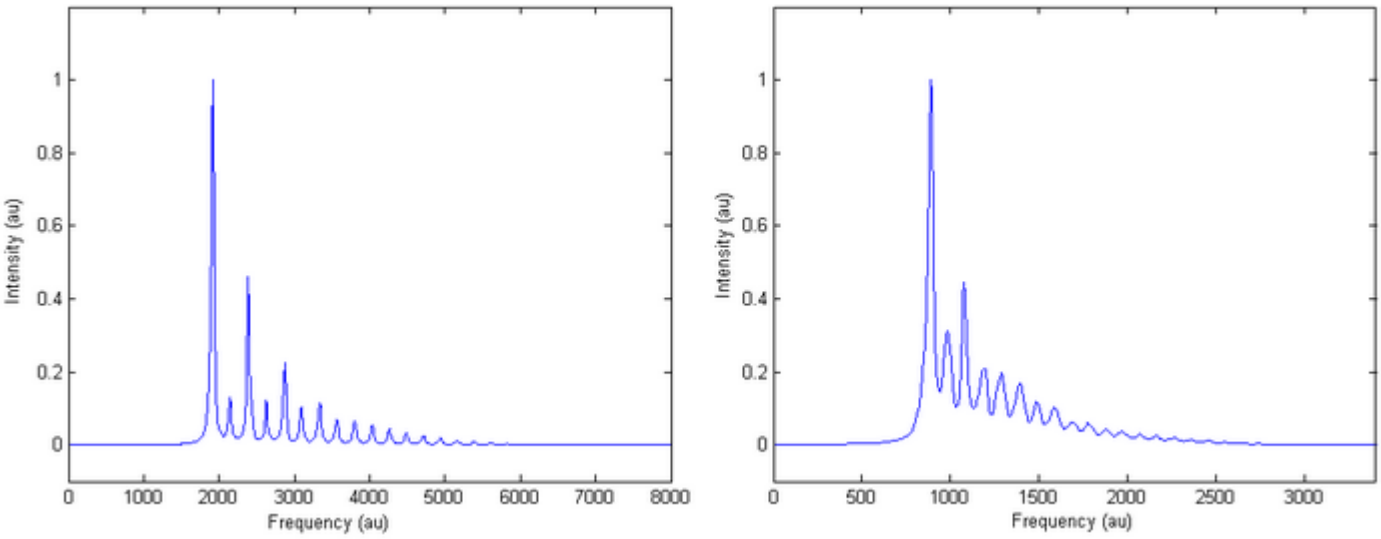

Figure 30: Transmission through the SFPI for two different configurations. On the left all modes are separated. On the right modes starts merging.

We succeed to align the SFPI but the finesse is not as good as expected because of losses introduce by the lens. Indeed the finesse of such a cavity can't be computed only with the reflectivity of mirrors. In general the FWHM is by:

$$FWHM = \frac{FSR}{2\pi b} \tag{10}$$

with 1/b is all intensity losses in one round trip inside the cavity. These losses include transmission of the mirrors and reflection of the lens. We suppose that all losses come from transmission of the mirrors and reflection of the lens. In our case, we have two mirrors with a reflectivity of 99.5 % and one lens with a reflectivity of

0.5 %.

$$Losses = T_1 + T_2 + 4 \cdot R_{lens} \tag{11}$$

with T_1, the transmission of the plan mirror, T_2, the transmission of the concave mirror and R_{lens}, the reflectivity of the lens. With these optics, we can expect a finesse of 205.

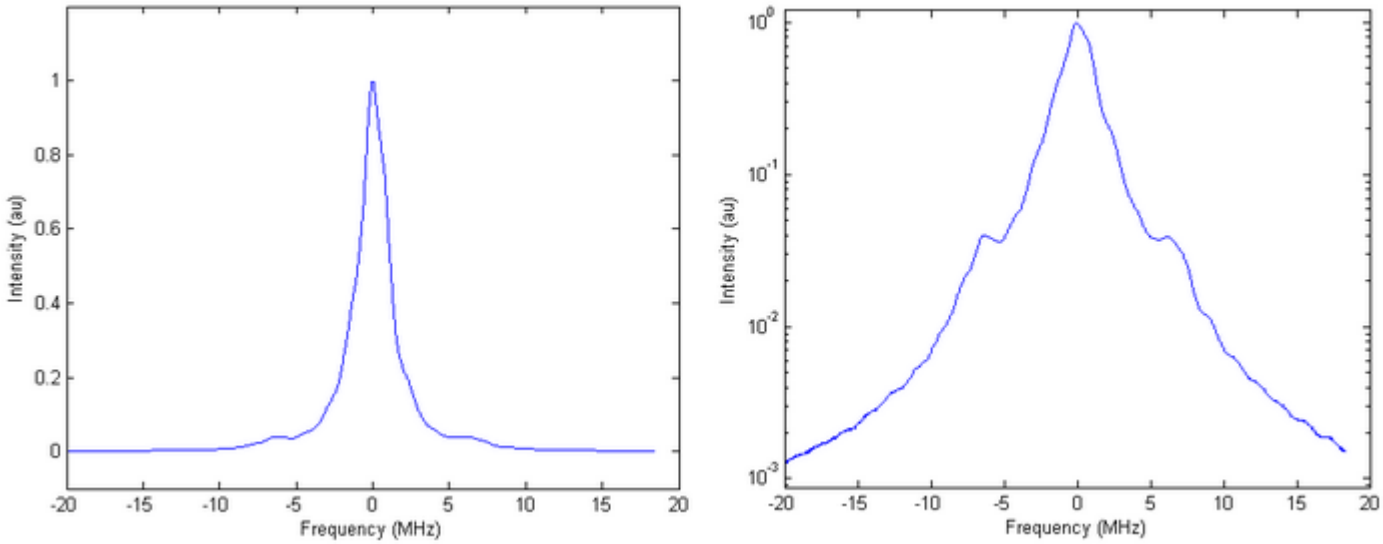

Figure 31: Preliminary results of the SFPI. Transmission through the SFPI in linear scale and logarithmic scale.

The FWHM measured in fig.31 is 2.18 MHz. Experimentally, we found a finesse of 105. Which is half than what we expect. It can be explained by a non optimal adjustment of the lengths or unexpected losses in optics.

4 Conclusion

In conclusion we success to build a SFP with a resolution good enough to resolve modulation sidebands used in VIRGO. Perspective for future works are to improve the alignment of the SFPI and try to increase the finesse of the cavity in order to be able to make an image of the sidebands. We also have to make an image of a target through the cavity and , then make an image of modulation sidebands. At some point, these cavities could be installed on VIRGO.

5 Annexes

Annex A

Technical drawing of the support for the piezo electric actuator we put on the mount.

Annex B

Technical drawing of the support for 2 inch mirror we put on the piezo actuator.

Annexes C and D

Technical drawing of the support for 1 inch mirror we put on the piezo actuator.

Annex E

Technical drawing of the 1 inch adapter for 2 inch mount.

Annexex F and G

Technical drawing of the box and the plate used to stabilize the SFP.

Annexes H and I

Technical drawing of the box and the plate used to stabilize the SFPI.

Annex J

Technical drawing of all supports and adapter in the optical mounts.

References

[1] R. W. P. Drever J. L. Hall, F. V. Kowalski and al. Laser phase and frequency stabilization using an optical resonator. *Applied Physics B*, vol. 31:pp 97–105, 1983.

[2] E. D. Black. An introduction to pound–drever–hall laser frequency stabilization. *American Association of Physics Teachers.*, 2001.

[3] The VIRGO Collaboration. *Advanced Virgo Technical Design Report*, apr 2012.

[4] E. D'Ambrosio and B. Kells. Asymmetry between the sidebands used for detecting gravitational waves in laser interferometric antennas. *Optical Society of America*, vol. 21, 2004.

[5] *VIRGO Logbook entry 18331 August 2007.*

[6] A. E. Siegman. *Laser*, 1986.

[7] B. E. A. Saleh and M. C. Teich. *Fundamentals of Photonics*, 1991.

[8] The VIRGO Collaboration. *The VIRGO Physics Book*, apr 2006.

[9] J. R. Johson. A method for producing precisely confocal resonators for scanning interferometers. *Applied Optics*, vol. 6, 1967.

[10] J. A. Arnaud. Degenerate optical cavities. *Applied Optics*, vol. 8(no. 1), 1969.

[11] B. Chalopin A. Chiummo, C. Fabre and al. Frequency doubling of low power images using a self-imaging cavity. *Opt. Express 18*, 2010.